Investigation of Jet Collimation using Astra

J. N. Waugh, C. D. Gregory* and L. A. Wilson
Department of Physics, University of York, York, YO10 5DD, UK

B. Loupias, E. Brambrink and M. Koenig
Laboratoire pour l'Utilisation des Lasers Intenses, UMR 7605, CNRS – CEA – Université Paris VI – Ecole Polytechnique, 91128 Palaiseau Cedex, France

Y. Sakawa, Y. Kuramitsu, H. Takabe and R. Kodama
Institute of Laser Engineering, Osaka University, Yamada Oka 2-6 Suita, Yamada Oka, Osaka 565-0871, Japan

N. C. Woolsey
Department of Physics, University of York, York, YO10 5DD, UK

Since the experiment C. D. Gregory has moved to LULI, Laboratoire pour l'Utilisation des Lasers Intenses, UMR 7605, CNRS – CEA – Université Paris VI – Ecole Polytechnique, 91128 Palaiseau Cedex, France

Contact | **jnw501@york.ac.uk**

Introduction

The experiment described in this report is part of an ongoing campaign to create scale models of astrophysical plasma jets in the laboratory using lasers in order to learn about their much larger counterparts (see [1] and [2] for examples of other experiments within the campaign). The plasma jets observed by astronomers vary greatly [3] in length, from the exceedingly large (over 1 MParsec), highly relativistic jets seen emerging from active galactic nuclei (AGN) down to the much smaller (only ~10-100 lightdays), non-relativistic jets associated with 'Young Stellar Objects' (YSOs). It is this latter class of jet that we attempted to simulate in this experiment.

AGN and YSO systems share a common structure: a rotating accretion disc encircles a massive object (a supermassive black hole in the case of AGN and a protostar in the case of YSOs) and perpendicular to this disc supersonic jets of plasma are expelled. These jets are observed to be highly-collimated (i.e. their length greatly exceeds their width). Several factors are thought to contribute to this. First, the jets are 'radiative'. This means that the timescale over which energy is lost via radiation is less than or comparable to the hydrodynamic timescale, or in other words that the rate at which the plasma loses energy by radiation is sufficient to have a significant impact on its bulk hydrodynamic motion: the more radiative a jet, the more rapidly the energy and hence pressure inside the jet reduce and so the greater the reduction in the lateral expansion that the internal pressure promotes. Second, though interstellar/intergalactic space is commonly considered to be a vacuum, when discussing jets space has rather to be regarded as a very low density plasma: the mass density of material in YSO jets is only ~10 times that in the surrounding space, and in the case of AGN the mass density within a jet is actually less than that of its surroundings [4]. The presence of the low-density plasma of space is expected to have an inertially confining effect on jets. Third, YSO and AGN systems (both the discs and the jets) have associated with them large-scale magnetic fields. It is thought that these fields are involved both in the launching and in the subsequent collimation of jets.

In the experiment, jets were created by firing the Astra laser (target area 2) into cones machined into solid blocks of aluminium alloy. It was expected that the target would work in the following fashion: the laser pulse would heat and ionise material from a thin coating layer put onto the surface of the cones. This material would then move away from the cone surface approximately along the surface normal, and hence would converge on the cone axis where its radial motion would arrest, leaving a mass of plasma moving along the cone axis – a jet. In addition to conical targets, flat targets were also shot, thus enabling it to be determined whether the convergence of plasma occurring when using conical targets was actually useful for jet creation.

With this basic method of jet creation two of the factors thought to affect jet collimation were investigated. In order to investigate the effect of radiation on jets. Jets were created from cones coated with materials of different atomic number. Higher atomic number ions radiate more efficiently within a plasma, so jets made from higher atomic number materials are more radiative and can be expected to form better collimated jets. In order to investigate the effect of inertial confinement on a jet, jets were created that propagated into a variety of different background gas pressures. Actually, changing the jet material is expected to have an effect on inertial confinement as well as on radiative efficiency: changing jet material results in a change of atomic number and also of atomic mass. As well as different pressures of background gas, different types of background gas were used. These gases, having different atomic numbers, would have different radiative efficiencies when ionised.

The jet creation method used in this experiment is similar to that used by Shigemori *et al* [5]. In that experiment laser shots were taken into cones made of several different materials using the GEKKO XII laser system, allowing a comparison between jets of different atomic number and hence exploring how radiative efficiency affected jet collimation: as expected, higher atomic number jets were seen to be better-collimated. There are several ways in which the experiment reported here adds information to that coming from Shigemori's experiment including (i) the jets created in this experiment propagated into background

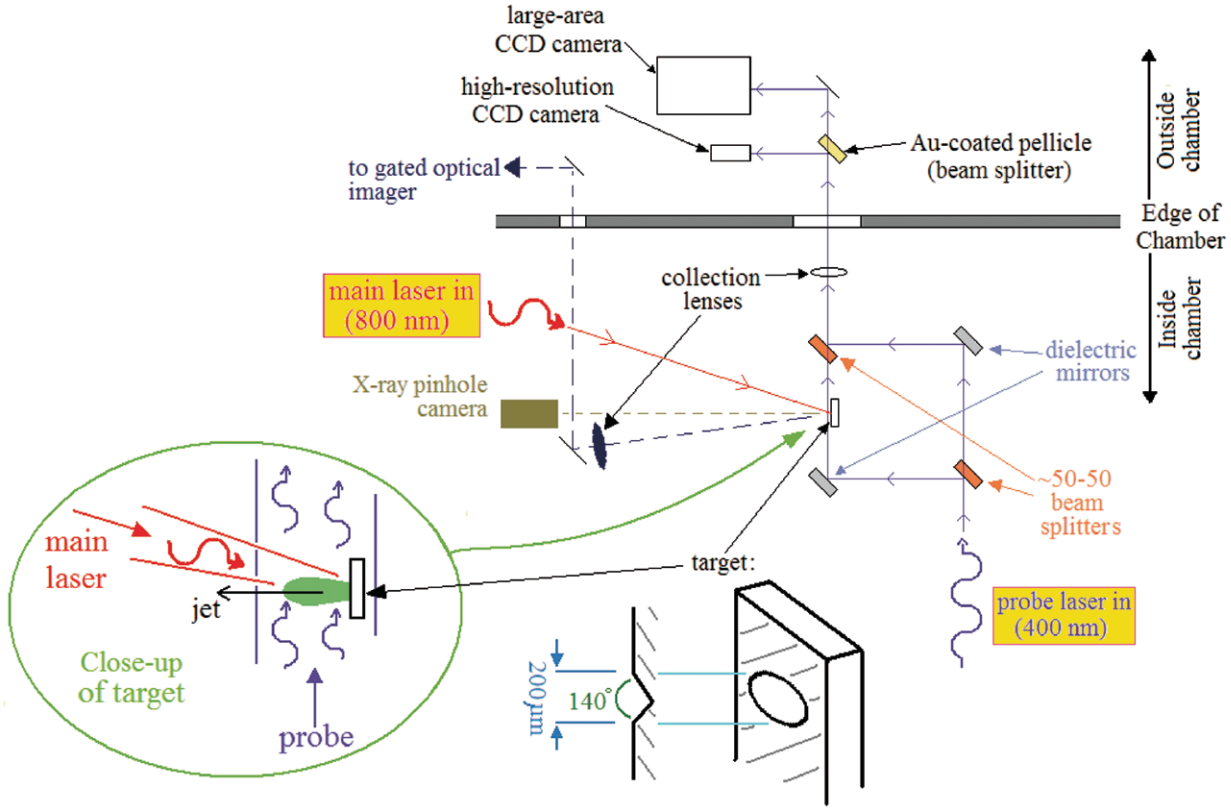

Figure 1. Experimental set-up. The main Astra beam comes in to the target at 8° to target normal. The probe beam passes the target perpendicular to target normal.

gases allowing investigation of inertial confinement (ii) the main diagnostic in this experiment was optical probe interferometry meaning electron density profiles can be found for jets of sufficient cylindrical symmetry.

Experimental details

The experimental set-up is shown in figure 1. The main Astra beam (pulse length ~2 ps, energy ~0.5 J, wavelength 800 nm and focal spot FWHM ~100 μm) came onto the target from an f/6.5, off-axis parabola with 8° degrees between target normal and the beam axis. While several target geometries were shot, the main target type was the 'dimple' target. These were made by machining a line of cones (each cone having diameter 200 μm and full opening angle 140°, with inter-cone separation 2 mm) into 5 cm long blocks of an aluminium alloy that had previously been lapped on the front surface. The machined blocks were given a thin coating of either plastic (specifically n-type polypropylene), Al, Cu, Cu-smoke or Au. The jets created by the laser-target interaction emerged into a static gas back-fill (i.e. the vacuum chamber in which the experiment was conducted was first pumped out and then filled with a pure bottled gas), either He, N_2 or Xe. A range of gas pressures was used, including vacuum (pressure ~10^{-4} mb).

Several diagnostics were used to observe the created jets, specifically interferometry, an X-ray pinhole camera and optical self-emission imaging. The optical probe interferometry was the main diagnostic. The probe beam (a part of the main Astra beam taken off after the second amplifier stage and frequency doubled to 400 nm with a pulselength of 50 fs) was sent through a Mach-Zehnder interferometer arranged in such a fashion that one of its arms was far from the target while the other passed the target front side; the created laser-plasma propagated into the path of this second arm. The probe light emerging from the second beam-splitter of the interferometer was collected and focused using an f/3 lens and, after exiting the vacuum chamber through a glass window anti-reflection soft-coated for 400 nm, the beam was split into two parts using a gold-coated pellicle. One part was focused onto a Basler CCD camera, the other onto an Andor CCD camera. Both cameras were filtered with 400 nm interference filters. The small pixel size (6.45 μm) of the Basler CCD meant this camera could be used to take high-resolution, small field of view images of the central regions of the jets, while the large chip size (2048×2048 pixels) of the Andor CCD meant it could be used to take lower resolution, large field of view (2.9×3.0 mm at the target position) images of the jets without having to change the magnification of the probe line before either camera.

The optical self-emission imaging was done by placing an ~f/3 collection lens approximately ~16 cm from the target at an angle of 9° with respect to target normal. The camera used was an Andor i-star (a gated CCD) filtered with a 632 nm interference filter and ND 2. As for the X-ray pinhole camera, the camera used was an Andor (direct exposure) CCD camera filtered with Be. No pinhole or self-emission data is presented in this paper.

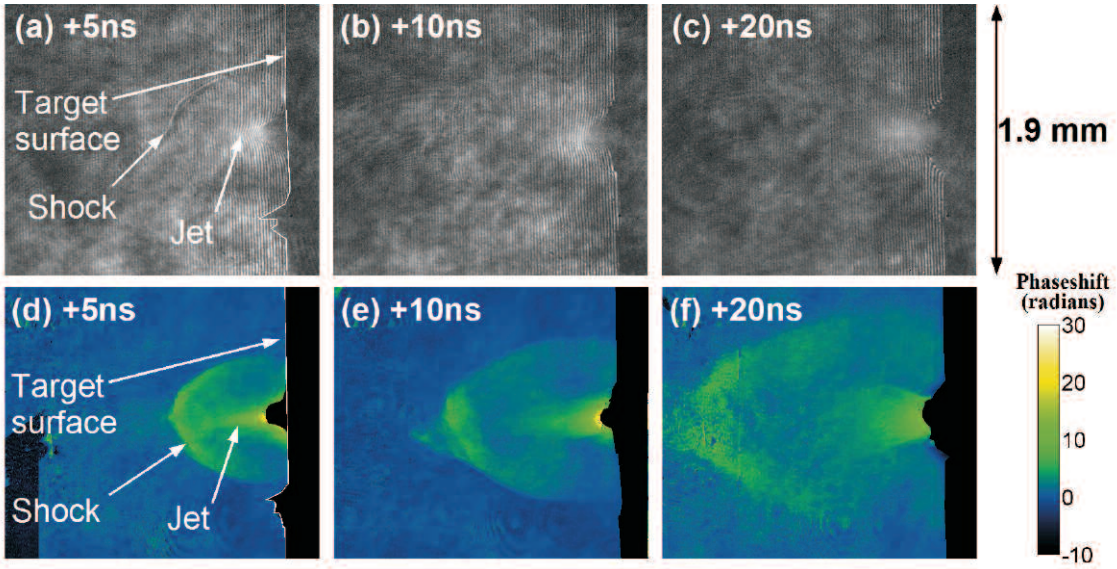

Figure 2. Partial time series for a copper plasma emerging into 50 mb Hw. (a)-(c) are interferograms recorded by the large-area CCD camera. (d)-(f) are phasemaps calculated from (a)-(c) respectively: they are two-dimensional maps of the shift in phase incurred by probe beam photons due to having to pass through the laser-plasma.

Results

Figure 2 shows some of the data from the experiment. Figure 2(a)-(c) are interferograms (raw interferometry data) and figure 2(d)-(f) are phasemaps calculated from 2(a)-(c). Figure 2(a) and (d) show the basic structure of the plasmas produced in the experiment. The main laser comes in from the left in these images, strikes the target (the vertical, fringeless region on the right of each image) and produces a plasma that propagates from right to left. Typically this plasma has two components – a jet propagating approximately along target normal is preceded by a shock wave moving through the gas. The shock and jet are supersonic, moving at a typical speed of order 100 kms^{-1}. The hydrodynamic timescale (the timescale over which the bulk flow of the plasma evolves) is of order 1ns. Figure 2(a)-(c), and therefore also figure 2(d)-(f), are a partial time series showing the evolution of a copper jet moving into 50 mb He gas. Due to the very short timescale of the plasma evolution, it was not possible to record multiple images of a single jet at different times (the large-area CCD read-out time was several minutes). Rather, time series were built up by creating a series of nominally identical jets and changing the delay of the probe pulse with respect to the main laser pulse between shots: as the probe pulselength of 50 fs was much less than the hydrodynamic timescale the probe images are effectively instantaneous snapshots of the plasma system. The exposure time of the large-area CCD was much longer than the plasma lifetime, with the result that in addition to the short pulse of light coming from the probe pulse the interferometry images also contain the time-integrated 400 nm self-emission signal from the plasma. This is visible as a glow around the jet position in figure 2(a)-(c). It can be seen from figure 2(d)-(f) that, while the shock is still very much in evidence after 20 ns, the on-axis jet feature seen after 5 ns is hardly visible after 10 ns and completely gone after 20 ns.

One feature observable in figure 2(e) is the break-up of the otherwise smooth shock front near target normal. As the main laser pulse was focused down onto the target from the parabola it would have ionised the gas in its path, leaving an expanding cone of plasma within the static gas back-fill. It is thought that the shock break-up occurs where the shock from the laser-target interaction interacts with the laser-ionised gas cone (Edens *et al.* discuss such an effect in [6]). It is worth remarking here for clarity that though the main laser pulse came onto the target at 8° to target normal, the orientation of the probe line was such that the projection of the cone of plasma would appear to be along target normal in the interferometry images.

It is worth describing here what phasemaps actually show. In figure 2(a)-(c) the jet and shock structures are visible as shifts in the fringe pattern from the pattern of evenly-spaced, parallel fringes seen in the absence of plasma in the interferometer arms. The fringe shifting in the presence of plasma occurs as the refractive index of the plasma is different to that of the static gas back-fill, resulting in a shift in phase of the probe pulse that passes through it (with respect to the plasma-free situation). Using a computer program called IDEA[7] it is possible to extract 2-dimensional maps of the phaseshift incurred by the probe in passing through the plasma, and this is what the phasemap images in figure 2(d)-(f) actually show.

In addition to introducing a shift in phase, the refractive index has another effect on the probe beam. The inhomogeneous nature of the plasma meant that its refractive index was also inhomogeneous, with the effect that photons in the probe beam were refracted – in figure 2(d) the effect of this can be seen as a dark patch at the base of the jet which is the result of the probe beam here being refracted out of the collection angle of the collecting lens. While phasemaps are useful for visualising the plasma structure, the analysis of the interferometry data can be taken a step further. The phaseshift of probe photons in passing through

the plasma is, if it is assumed that refraction is negligible (which we have seen breaks down within some regions of the plasma), related to the line-integral along straight paths of a function of the plasma refractive index. As the refractive index is a function of probe wavelength (known to be 400 nm) and plasma electron density, the phasemaps are therefore effectively maps of line-integrated electron density. Using a numerical implementation of the mathematical procedure known as Abel inversion (for one possible approach to this see) it is possible to extract maps of the electron density within the plasma from the phasemaps. The Abel inversion procedure works on the assumption that the plasma system has some cylindrical symmetry, and repeats the use of the assumption that probe refraction by the plasma is negligible. For the experimental data extraction of electron density maps has yet to be completed.

The interferograms and phasemaps show that supersonic jets and shocks were produced in the experiment. However, it has to be asked whether, and how well, these jets serve as scale models of YSO jets. The microphysics underlying astrophysical and laboratory jets is in general different (for example, the dominant radiative emission process). However, the bulk motion of these two kinds of jet can, provided certain criteria are met, be described by the same set of (magneto-)hydrodynamic equations. In this case, a direct scaling between the two systems may be possible via the Euler relations (see[9]): if at some time the two systems are geometrically similar and take the same value of a quantity known as the Euler parameter, the systems evolve identically (to within scaling factors) after this. Strictly, this scaling relationship is only valid when the plasmas being described are dissipationless (i.e. they have negligible thermal conductivity, negligible viscosity, emit negligible amounts of energy via radiation etc.). However, astrophysical jets are radiative (the timescale for energy loss via radiation is short or comparable to the hydrodynamic timescale). The result of this is that the scaling between laboratory jets and YSO jets is only approximate. The quality of the approximation is judged by how well a set of scaling parameters calculated for the laboratory jets matches the values of the scaling parameters of YSOs calculated from observations. The relevant scaling parameters (see[9], and[10] which refers to[11]) are M_{int} (the jet internal Mach number, equal to the ratio of the bulk flow speed of the plasma inside the jet to the sound speed appropriate to the plasma inside the jet), η (the ratio of the mass density of the plasma in the jet to the mass density of the surrounding medium), χ (the ratio of the radiative cooling lengthscale of the jet plasma to the jet radius), Re (the Reynold's number – the ratio of the strengths of the inertial forces and the viscous forces within the plasma) and Pe (the Peclet number – a ratio indicating the importance of heat convection with respect to heat conduction). The values of the scaling parameters for the experiment have not yet been inferred, so it cannot yet be said whether, and how well, the laboratory jets model astrophysical jets.

Conclusions

In the experiment reported here supersonic plasma jets and shock waves were created, the shock speed being of order 100 kms^{-1}. It is still to be determined whether, or to what extent, the experimental jets are scale models of YSO jets.

In future experiments, two improvements on the astrophysical jet modelling in particular are being considered. The first of these relates to the medium the jets emerge into. YSO jets emerge into the interstellar medium, a plasma, but in the experiment described in this paper, the jets emerged into a gas. One way to improve the jet simulation is simply to ionise the gas in the immediate vicinity of the target just before the laser pulse. The second jet modelling improvement relates to magnetic fields. YSO systems are believed to be threaded by large-scale magnetic fields. It is planned in our next jet experiment to introduce a magnetic field using a pulsed electromagnet.

Acknowledgements

Thanks is expressed to the staff of the CLF, and we acknowledge provision of funding for the experiment from EPSRC, STFC, the Royal Society and JSPS. In addition, C. D. Gregory, who has moved to the LULI laboratory (Paris, France) since the experiment was performed, wishes to acknowledge current funding support from Région Ile-de-France.

References

1. C. D. Gregory, J. Howe, B. Loupias, S. Myers, M. M. Notley, Y. Sakawa, A. Oya, R. Kodama, M. Koenig, N. C. Woolsey, *ApJ*, **676**, 420-426 (2008).
2. B. Loupias, E. Falize, C. D. Gregory, O. Akira, T. Vinci, J. Howe, M. Koenig, N. C. Woolsey, N. Ozaki, A. Benuzzi-Mounaix, S. Bouquet, C. Michaut, M. Rabec le Goahec, W. Nazarov, T. Pikuz, A. YA. Faenov, Y. Aglitskiy, S. Atzeni, A. Schiavi, Y. Sakawa, H. Takabe, R. Kodama, IFSA 2007, *Journal of Physics: Conference Series*, **112**, 042022 (2008).
3. E. M. de Gouveia Dal Pino, *AIP Conf. Proc.*, **784**, 183-194 (2005).
4. E. M. de Gouveia Dal Pino, *Advances in Space Research*, **35**, 5, 908-924 (2005).
5. K. Shigemori, R. Kodama, D. R. Farley, T. Koase, K. G. Estabrook, B. A. Remington, D. D. Ryutov, Y. Ochi, H. Azechi, J. Stone, N. Turner, *Phys. Rev. E*, **62**, 6, 8838-8841 (2000).
6. A. D. Edens, T. Ditmire, J. F. Hansen, M. J. Edwards, R. G. Adams, P. Rambo, L. Ruggles, I. C. Smith, J. L. Porter, *PoP*, **11**, 11, 4968-4972 (2004).
7. M. Hipp, J. Woisetschlager, P. Reiterer, T. Neger, *Measurement*, **36**, 53-66 (2004).
8. K. Bockasten, *J. Opt. Soc. Am.*, **51**, 9, 943-7 (1961).
9. D. Ryutov, R. P. Drake, J. Kane, E. Liang, B. A. Remington, W. M. Wood-Vasey, *ApJ*, **518**, 821-832 (1999).
10. S. V. Lebedev, J. P. Chittenden, F. N. Beg, S. N. Bland, A. Ciardi, D. Ampleford, S. Hughes, M. G. Haines, A. Frank, E. G. Blackman, T. Gardiner, *ApJ*, **564**, 113-119 (2002).
11. J. M. Blondin, B. A. Fryxell, A. Konigl, *ApJ*, **360**, 370-386 (1990).